

Discovery of Radio Emission from the Brown Dwarf LP944–20

E. Berger¹, S. Ball², K. M. Becker³, M. Clarke⁴, D. A. Frail⁵, T. A. Fukuda⁶, I. M. Hoffman⁷, S. R. Kulkarni¹, R. Mellon⁸, E. Momjian⁹, N. W. Murphy¹⁰, S. H. Teng¹¹, T. Woodruff¹², B. A. Zauderer¹³, R. T. Zavala¹⁴

¹ Division of Physics, Mathematics & Astronomy 105-24, California Institute of Technology, Pasadena, CA 91125, USA

² Department of Physics, New Mexico Tech, PO Box 3394 c/s, Socorro, NM 87801

³ Department of Physics, Oberlin College, Oberlin, OH 44074

⁴ Department of Physics, Carleton College, 300 N. College St., Northfield, MN 55057

⁵ National Radio Astronomy Observatory, P. O. Box O, Socorro, NM 87801, USA

⁶ Department of Physics & Astronomy, University of Denver, 2112 E. Wesley Ave., Denver, CO 80208

⁷ Department of Physics & Astronomy, University of New Mexico, 800 Yale Blvd. NE, Albuquerque, NM 87131

⁸ Department of Astronomy, 525 Davey Lab., The Pennsylvania State University, University Park, PA 16802

⁹ Department of Physics & Astronomy, 177 chem-physics building, University of Kentucky, Lexington, KY 40506

¹⁰ Department of Physics, Amherst College, Amherst, MA 01002-5000

¹¹ Department of Astronomy, Univeristy of Maryland, College Park, MD 20742

¹² Department of Physics, Southwestern University, S.U. Box 7263, Georgetown, TX 78626

¹³ Department of Physics & Astronomy, Agnes Scott College, Decatur, GA 30030

¹⁴ Department of Astronomy, New Mexico State University, MSC 4500 PO Box 30001, Las Cruces, NM 88003

Brown dwarfs are classified as objects which are not massive enough to sustain nuclear fusion of hydrogen, and are distinguished from planets by their ability to burn deuterium.¹ Old (>10 Myr) brown dwarfs are expected to possess short-lived magnetic fields² and, since they no longer generate energy from collapse and accretion, weak radio and X-ray emitting coronae. Several efforts have been undertaken in the past to detect chromospheric activity from the brown dwarf LP944–20 at X-ray^{1,3} and optical^{4,5,6,7} wavelengths, but only recently an X-ray flare from this object was detected.³ Here we report on the discovery of quiescent and flaring radio emission from this source, which represents the first detection of persistent radio emission from a brown dwarf, with luminosities that are several orders of magnitude larger than predicted from an empirical relation^{8,9} between the X-ray and radio luminosities of many stellar types. We show in the context of synchrotron emission, that LP944–20 possesses an unusually weak magnetic field in comparison to active dwarf M stars,^{10,11} which might explain the null results from previous optical and X-ray observations of this source, and the deviation from the empirical relations.

This paper has been submitted to Nature. You are free to use the results here for the purpose of

your research. In accordance with the editorial policy of Nature, we request that you not discuss this result in the popular press. If you have any question or need clarifications please contact Edo Berger, ejb@astro.caltech.edu.

Following the detection of an X-ray flare from the brown dwarf LP944–20 on 1999 December 15 by the *Chandra* X-ray Observatory,³ we observed the X-ray position of this source with the Very Large Array (VLA) on 2000 July 27.54 UT, and detected a radio source. We tested the radio emission for variability by imaging subsets of the observation and constructing a light-curve, and found a bright flare, as well as quiescent emission (see Figure 1). In subsequent observations we detected two additional flares, and quiescent emission at 4.9 and 8.5 GHz. A log of all observations, the details of the data reduction, and results can be found in Table 1 and Figure 1. The quiescent emission at the location of the source was detected at the $2-3\sigma$ level in individual measurements, but with a level of 2.5 and 5.5 σ for the average of all measurements at 4.9 and 8.5 GHz, respectively. Since we know the precise location of the source, these levels represent a significant detection of quiescent emission.

This set of observations comprises the first detection of persistent quiescent and flaring emission from a bona-fide brown dwarf.^{1,12} Moreover, the levels of emission — approximately 80 μ Jy in quiescence and 2 mJy at peak-flare — are highly unusual in the context of stellar coronal emission. We now seek to interpret the quiescent and flaring emission in this framework.

Coronal activity in a broad range of stars has been studied by Guedel and Benz who found⁸ a simple empirical relation between the quiescent X-ray and radio luminosities, $L_R \approx L_X/10^{15.5} \text{ Hz}^{-1}$. Using this relation with the *Chandra*-determined³ upper limit on the quiescent X-ray luminosity of LP944–20, $L_X < 10^{24} \text{ erg sec}^{-1}$ (0.1 – 10 keV band), we find that the expected quiescent radio luminosity is $L_R < 3.5 \times 10^8 \text{ erg sec}^{-1} \text{ Hz}^{-1}$, which translates to a received flux density of $< 0.01 \mu$ Jy on Earth. Therefore, the flux density we measured in quiescence is at least four orders of magnitude larger than predicted.

Benz and Guedel also found⁹ a similar, but slightly non-linear, relation between X-ray and radio flares from a broad range of stars. The non-linearity means that for flaring emission the ratio L_X/L_R varies with the luminosity of the flare. For the X-ray luminosity detected by *Chandra*, $L_X \approx 1.2 \times 10^{26} \text{ erg sec}^{-1}$, the relation is $L_X/L_R \approx 10^{16.5} \text{ Hz}$, and we therefore predict an observed radio flux density, $F_{\nu R} \approx 0.1 \mu$ Jy. The actual observed value is approximately 2×10^4 times higher.

Even though the X-ray and radio observations were not carried simultaneously, X-ray flares bright enough to resolve the discrepancy are not likely. In order to conform to the Benz–Guedel relation, the luminosity of the X-ray flares would have to be approximately equal to the bolometric luminosity of LP944–20. Such superflaring activity^{13,14} has been observed in nine *solar*-type stars, but with an average recurrence time of years to centuries. In contrast, the average recurrence time for the radio flares is of order several hours (see Table 2). Moreover, with such a short recurrence time, *Chandra* would have been expected to detect at least one of these superflares during the 13-hour observation of LP944–20. We can therefore conclude that the Benz–Guedel relation for flaring emission is severely violated, and the radio emission from LP944–20 is highly abnormal when compared to stellar emission.

The brightness temperature of the radio emission, approximately 2×10^8 K in quiescence and 4×10^9 K during flares, indicates that the emission mechanism is non-thermal. Most likely the emission is via synchrotron, which comes from relativistic electrons gyrating in a magnetic field and emitting radio waves at high harmonics of the electron gyrofrequency. Another possible mechanism is coherent emission, but the observed properties of the quiescent and flaring emission: flare timescale of order minutes, polarization of order 30%, broad-band emission, and $T_b < 10^{10}$ K, all point to synchrotron emission;^{11,15} for coherent emission we would expect a much shorter timescale, a much higher polarization and brightness temperature, and narrow-band emission. For a comprehensive treatment of synchrotron theory we refer the reader to the work of Rybicki and Lightman.¹⁶

To find the spectral properties of the flaring emission, and thus the physical properties of the emission region around LP944–20, we use the observed fraction of circular polarization in the flaring emission at 8.5 GHz, $f_{\text{circ}} = 0.3 \pm 0.1$, which matches theoretical predictions^{17,18,19} for optically-thin synchrotron emission at moderate values of the gyrating electrons’ minimum Lorentz factor (γ_{min}). In addition, we find from the simultaneous observation on 2000 August 30.40 UT that the spectral index between 4.9 and 8.5 GHz was 2.1 ± 0.3 , indicating that the emission at 4.9 GHz was optically-thick (see Figure 1c). We therefore conclude that the radio spectrum of the flaring emission peaks at about 8.5 GHz, so that most of the energy in the flares at radio wavelengths is released at this frequency. Thus, we can use $\nu_{\text{peak}} = 8.5$ GHz and $F_\nu(8.5\text{GHz}) \equiv F_{\nu,\text{peak}}$ as an excellent approximation for the flare energetics (see Table 2).

The amount of energy released in the flares is estimated by using an exponentially rising and

decaying model, and solving for the peak flux density and rise and decay times (see Table 2). We find that the energy released in each of the flares at radio wavelengths is approximately the same, ranging from $2 - 8 \times 10^{26}$ ergs. Interestingly, this energy release is several times larger than for the brightest solar flares.¹⁸ From the flare model we also find that the best-fit quiescent flux density is $100 \pm 35 \mu\text{Jy}$, and that the probability of no quiescent component is 2×10^{-4} . This result serves to bolster our claim that we detected quiescent emission at a level of $100 \mu\text{Jy}$ from LP944–20.

From the fraction of circular polarization we can also estimate the value of γ_{min} using the relation for synchrotron emission $f_{\text{circ}} \approx 3/\gamma_{\text{min}}$, which gives $\gamma_{\text{min}} \approx 10$. Using the more accurate formalism of Dulk and Marsh,¹⁹ we get a similar result.

With the values of γ_{min} , ν_{peak} , and $F_{\nu, \text{peak}}$ we now calculate the magnetic field strength and the electron density during a flare from the basic equations of synchrotron theory,¹⁶ and from the minimum energy argument, which relies on the premise that the energy of a source is minimized in equipartition.^{20,21} From synchrotron theory we find that the magnetic field strength is $B \approx 5$ G, and the total number of electrons is $N_e \approx 2 \times 10^{35}$ (see Figure 1). From equipartition we find that the “equipartition radius”²² of LP944–20 is $\theta_{eq} \approx 75 \mu\text{as}$, while its physical angular size is $\theta_s \approx 60 \mu\text{as}$, indicating that the energy is released from a thin shell around the source, with a volume, $V \approx 4 \times 10^{29} \text{ cm}^3$. The electrons’ Lorentz factor calculated from equipartition is $\gamma_{\text{min}} \approx 10$, which is exactly the value we calculated independently from circular polarization, and hence we again find that $B \approx 5$ G and $N_e \approx 2 \times 10^{35}$. Using the volume of the emitting shell we calculate an electron number density, $n_e \approx 6 \times 10^5 \text{ cm}^{-3}$. For comparison, the surface magnetic field of Jupiter²³ is approximately 10 G, while in Solar flaring emission¹⁷ the magnetic field is $B \sim 80$ G, but the electron density and energy are much lower than in the flaring emission from LP944–20.

Similarly, the magnetic fields of some active dwarf M stars^{10,11} reach strengths of a few kG, and their X-ray luminosities *in quiescence*^{24,25,26} are of order $10^{27} - 10^{29} \text{ erg sec}^{-1}$. These are markedly different conditions than those in and around LP944–20, as evidenced by the weak magnetic field and non-detectable quiescent X-ray emission, but they may help to elucidate several lines of evidence that point to no magnetic field activity in this object. Extremely low levels of H α emission,⁵ which indicate no chromospheric activity, rapid rotation,⁵ which indicates no magnetic braking, and relatively old age,⁴ which implies a quenched dynamo mechanism, all agree with a magnetic field strength of a few Gauss rather than the much stronger fields observed in M dwarfs, the Sun, and even Jupiter.

We finally note that radio synchrotron and X-ray emission are expected in the context of a basic model of coronal emission — the magnetic reconnection process,^{18,27} and that the previously noted constancy of radio-wavelength energy release during flares appears to indicate that magnetic reconnection in LP944–20 takes place once the magnetic fields reach a critical strength, and therefore release approximately the same amount of energy every time.

It is still not clear why the emission from LP944–20 violates the Guedel–Benz relations so severely, but it is possible that this violation is tied to the difference in physical conditions in LP944–20 relative to M dwarfs, namely a very weak magnetic field. It is therefore crucial that radio and X-ray observations of this and other brown dwarfs be undertaken in order to establish whether similar conditions and unusually strong radio emission are common to some of these objects. In particular, it is clear that the radio regime is highly effective for detailed studies of both the flaring and quiescent emission due to the ease and availability of radio observations and the excellent sensitivity of radio telescopes.

Received 31 August 2018; Accepted .

1. Neuhäuser, R., Briceño, C., Comerón, F., Hearty, T., Martín, E. L., Schmitt, J. H. M. M., Stelzer, B., Supper, R., Voges, W. & Zinnecker, H. Search for X-ray emission from bona-fide and candidate brown dwarfs. *Astr. Astrophys.* **343**, 883–893 (1999).
2. Durney, B. R., De Young, D. S. & Roxburgh, I. W. On the generation of the large-scale and turbulent magnetic fields in solar-type stars. *Solar Phys.* **145**, 207–225 (1993).
3. Rutledge, R. E., Basri, G., Martín, E. L. & Bildsten, L. Chandra Detection of an X-Ray Flare from the Brown Dwarf LP 944-20. *Astrophys. J.* **538**, L141–L144 (2000).
4. Tinney, C. G. The intermediate-age brown dwarf LP944-20. *Mon. Not. R. astr. Soc.* **296**, L42–L44 (1998).
5. Tinney, C. G. & Reid, I. N. High-resolution spectra of very low-mass stars. *Mon. Not. R. astr. Soc.* **301**, 1031–1048 (1998).
6. Tinney, C. G. & Tolley, A. J. Searching for weather in brown dwarfs. *Mon. Not. R. astr. Soc.* **304**, 119–126 (1999).
7. Kirkpatrick, J. D., Henry, T. J. & Irwin, M. J. Ultra-Cool M Dwarfs Discovered by QSO Surveys.I: The APM Objects. *Astron. J.* **113**, 1421–1428 (1997).
8. Guedel, M. & Benz, A. O. X-ray/microwave relation of different types of active stars. *Astrophys. J.* **405**, L63–L66 (1993).
9. Benz, A. O. & Guedel, M. X-ray/microwave ratio of flares and coronae. *Astr. Astrophys.* **285**, 621–630 (1994).
10. Saar, S. H. & Linsky, J. L. The photospheric magnetic field of the dM3.5e flare star AD Leonis. *Astrophys. J.* **299**, L47–L50 (1985).
11. Haisch, B., Strong, K. T. & Rodono, M. Flares on the sun and other stars. *Ann. Rev. Astr. Ap.* **29**, 275–324 (1991).
12. Krishnamurthi, A., Leto, G. & Linsky, J. L. A Search for Radio Emission at the Bottom of the Main Sequence and Beyond. *Astron. J.* **118**, 1369–1372 (1999).
13. Schaefer, B. E., King, J. R. & Deliyannis, C. P. Superflares on Ordinary Solar-Type Stars. *Astrophys. J.* **529**, 1026–1030 (2000).

14. Rubenstein, E. P. & Schaefer, B. E. Are Superflares on Solar Analogues Caused by Extrasolar Planets? *Astrophys. J.* **529**, 1031–1033 (2000).
 15. Dulk, G. A. in *LNP Vol. 291: Cool Stars, Stellar Systems and the Sun* (eds Linsky, J. L. & Stencel, R. E.) 72–82 (Berlin, Springer–Verlag, 1987. 537 p., 1987).
 16. Rybicki, G. B. & Lightman, A. P. *Radiative processes in astrophysics*. New York, Wiley-Interscience, 1979. 393 p. (1979).
 17. Bruggmann, G. & Magun, A. Temporal and spectral characteristics of the circular polarization of solar microwave bursts. *Astr. Astrophys.* **239**, 347–355 (1990).
 18. Bastian, T. S., Benz, A. O. & Gary, D. E. Radio Emission from Solar Flares. *Ann. Rev. Astr. Ap.* **36**, 131–188 (1998).
 19. Dulk, G. A. & Marsh, K. A. Simplified expressions for the gyrosynchrotron radiation from mildly relativistic, nonthermal and thermal electrons. *Astrophys. J.* **259**, 350–358 (1982).
 20. Burbidge, G. R. & Burbidge, E. M. The Sources of Radio Emission in NGC 5128 and NGC 1316. *Astrophys. J.* **125**, 1–8 (1957).
 21. Readhead, A. C. S. Equipartition brightness temperature and the inverse Compton catastrophe. *Astrophys. J.* **426**, 51–59 (1994).
 22. Scott, M. A. & Readhead, A. C. S. The low-frequency structure of powerful radio sources and limits to departures from equipartition. *Mon. Not. R. astr. Soc.* **180**, 539–550 (1977).
 23. Smith, E. J., Davis, L., Jones, D. E., Coleman, P. J., Colburn, D. S., Dyal, P. & Sonett, C. P. Jupiter’s magnetic field, magnetosphere, and interaction with the solar wind - Pioneer 11. *Science* **188**, 451–455 (1975).
 24. Fleming, T. A., Liebert, J., Gioia, I. M. & Maccacaro, T. M dwarfs from the Einstein extended medium sensitivity survey. *Astrophys. J.* **331**, 958–973 (1988).
 25. Giampapa, M. S., Rosner, R., Kashyap, V., Fleming, T. A., Schmitt, J. H. M. M. & Bookbinder, J. A. The Coronae of Low-Mass Dwarf Stars. *Astrophys. J.* **463**, 707–725 (1996).
 26. Fleming, T. A., Giampapa, M. S., Schmitt, J. H. M. M. & Bookbinder, J. A. Stellar coronae at the end of the main sequence - A ROSAT survey of the late M dwarfs. *Astrophys. J.* **410**, 387–392 (1993).
 27. Sturrock, P. A. Chromospheric Magnetic Reconnection and Its Possible Relationship to Coronal Heating. *Astrophys. J.* **521**, 451–459 (1999).
-

Acknowledgements

We thank B. Clark for the allocation of ad hoc VLA time. We also thank D. E. Gary and R. Sari for helpful discussions. The initial observation of LP944–20 was undertaken as part of the National Radio Astronomy Observatory (NRAO) VLA Summer Program funded by the National Science Foundation (NSF). The National Radio Astronomy Observatory is a facility of the NSF operated under cooperative agreement by Associated Universities, Inc.

Date (UT)	Frequency (GHz)	On-source observation time (ksec)	Synthesized beam size (arcsec)	$F \pm \sigma$ (μJy)
2000 July 27.54	8.46	3.6	26.6×6.4	300 ± 45
2000 Aug 11.47	8.46	4.2	27.5×7.0	70 ± 27
2000 Aug 15.45	4.86	1.7	52.6×12.6	127 ± 53
2000 Aug 15.45	8.46	1.6	29.8×7.1	130 ± 44
2000 Aug 23.43	8.46	5.6	27.2×7.3	250 ± 26
2000 Aug 30.40	4.86	7.2	41.4×12.6	106 ± 50
2000 Aug 30.40	8.46	7.2	26.5×7.6	323 ± 49
2000 Sep 6.39	8.46	8.8	22.9×6.2	70 ± 39
2000 Sep 6.39	22.5	8.8	10.4×4.4	190 ± 170
2000 Sep 20.34	4.86	10.5	33.9×13.7	50 ± 36
2000 Sep 20.34	8.46	10.5	45.5×6.6	140 ± 45
2000 Sep 27.35	8.46	10.2	22.9×7.4	53 ± 20

Table 1. A summary of VLA observations of LP944–20, exhibiting both quiescent and flaring emission. The columns are (left to right), (1) UT date of the start of each observation, (2) observing frequency, (3) On-source observing time, (4) Synthesized beam size, and (5) peak flux density at the best fit position of LP944–20, with the error given as the root mean square noise on the image. Single-frequency observations consisted of several on-source scans using the VLA standard continuum mode, with the full 100 MHz bandwidth obtained in two adjacent 50 MHz bands. The flux density scale was determined using the extra-galactic source 3C48 (J0137+331), and the phase was monitored using the sources J0334–401 and J0403–360. Dual-frequency observations were done with a split array configuration in which only several antennas were used for each observing frequency. The data were reduced with the Astronomical Image Processing System (AIPS, releases 15APR1999 and 31DEC1999).

In the initial observation we detected an object with a flux $F_{8.5\text{GHz}} = 300 \pm 45 \mu\text{Jy}$ at $\alpha(\text{J2000})=03^{\text{h}}39^{\text{m}}35.3^{\text{s}}$, $\delta(\text{J2000})=-35^{\circ}25'44.0''$, with an error of $\sim 1''$ in both α and δ . We identify our detection with the brown dwarf LP944–20 based on the positional coincidence between this detection and the X-ray position³ provided by *Chandra*.

Parameter	2000 July 27.5727	2000 Aug 23.4407	2000 Aug 30.4849
F_0 (mJy)	1.5 ± 0.1	2.6 ± 0.2	2.0 ± 0.2
τ_1 (min)	$3.0^{+4.2}_{-1.5}$	$6.2^{+1.5}_{-0.8}$	20 ± 5
τ_2 (min)	$5.7^{+2.4}_{-1.6}$	$1.7^{+0.4}_{-0.3}$	$5.1^{+2.2}_{-1.5}$
δt_0 (min)	± 1	± 1	± 2
E_R (10^{26} ergs)	$2.0^{+1.5}_{-0.7}$	$3.1^{+0.8}_{-0.5}$	$7.7^{+2.3}_{-2.1}$

Table 2. A summary of the model parameters characterizing each of the observed flares. The flares were modeled using the equation: $F(t) = F_0 e^{(t-t_0)/\tau_1} + F_q$ for $t < t_0$ and $F(t) = F_0 e^{-(t-t_0)/\tau_2} + F_q$ for $t \geq t_0$, where F_0 is the peak flux density, F_q is the quiescent flux of the source, and τ_1 and τ_2 are the rise and decay times, respectively. With this approach F_0 , t_0 , τ_1 , τ_2 , and F_q are free parameters, and the total value of χ^2 for all three flares is 3.7 for 9 degrees of freedom. Forcing F_q to have the same value at all times, we find that the level of quiescent emission derived from the model-fit is consistent with the quiescent flux densities measured during observations of non-flaring emission; from modeling we find an average quiescent flux of $100 \pm 35 \mu\text{Jy}$, while direct observations of the quiescent emission give a value of $75 \pm 23 \mu\text{Jy}$.

The energy released in the flares at radio wavelengths is calculated using the equation $E_R = 4\pi d^2 \nu_{\text{peak}} F_{\nu_{\text{peak}}} \tau$, where $d = 5$ pc is the distance to the source, $\nu_{\text{peak}} \approx 8.5 \times 10^9$ Hz is the peak frequency, $F_{\nu_{\text{peak}}}$ is the peak flux density in units of $\text{erg sec}^{-1} \text{cm}^{-2} \text{Hz}^{-1}$, and $\tau = \tau_1 + \tau_2$ is the temporal extent of the flare. We find that all three flares released approximately the same amount of energy at 8.5 GHz.

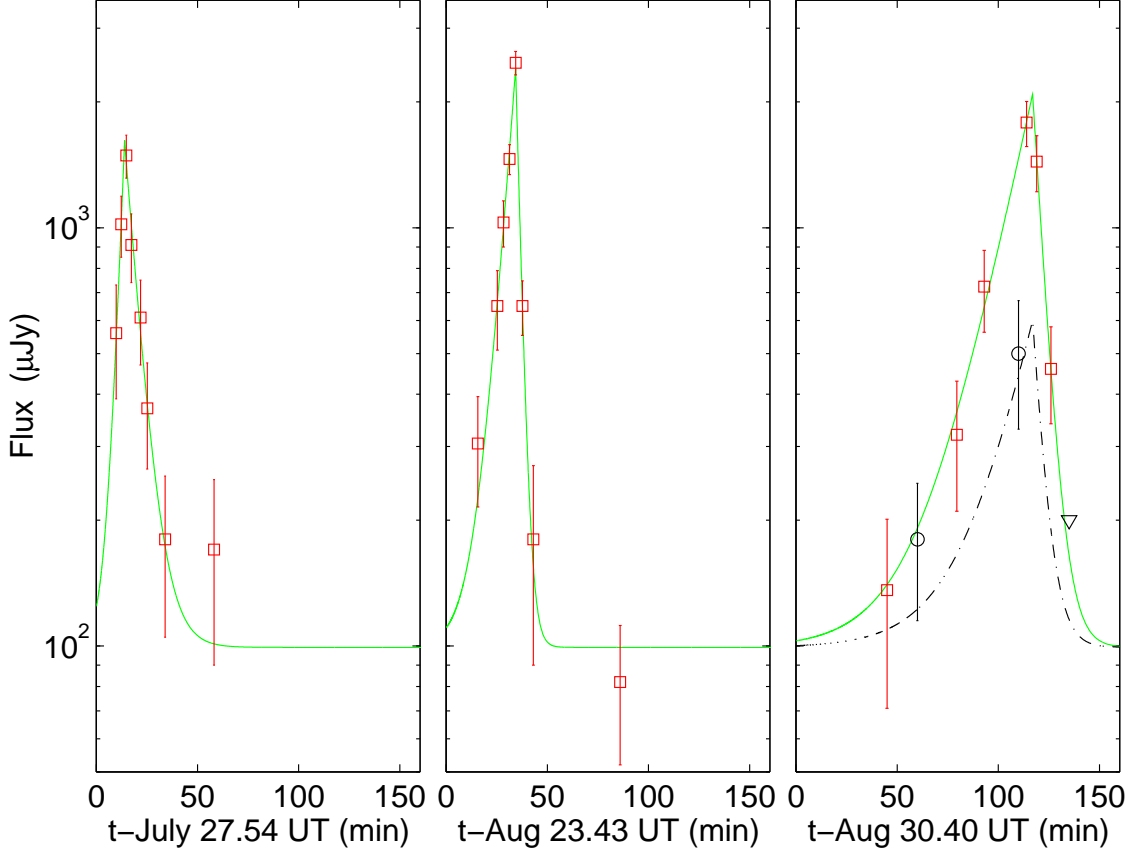


Figure 1. Light curves for the flaring radio emission from LP944–20 at 8.5 GHz (squares) showing strong flares, quiescent emission, and the self-absorbed emission at 4.9 GHz (circles; upper limit is given by an inverted triangle). The three panels are the lightcurves on (a) 2000 July 27.54, (b) 2000 August 23.43, and (c) 2000 August 30.40. Time in minutes is relative to the starting time of each observation, and the solid line is the model fit based on the fitting equation given in Table 2. Panel (c) also shows the flux density at 4.9 GHz, which was measured simultaneously with the 8.5 GHz observation. Based on the ratio of the flux densities at these two frequencies we find that the spectral index is 2.1 ± 0.3 , which indicates that the emission at 4.9 GHz is self-absorbed. The dashed line is a model fit based on the simple model (see notes Table 2) and the spectral shape of optically-thick synchrotron emission, $F_\nu \propto \nu^{5/2}$.

Based on these lightcurves we can calculate the magnetic field strength and the number density of trapped electrons using the equations for synchrotron emission: $\frac{eB}{m_e c} \gamma_e^2 = \nu \approx 8.5\text{GHz}$ and $\frac{4}{3} \sigma_T c \gamma_e^2 \frac{B^2}{8\pi} N = 4\pi d^2 \nu F_{\nu\text{peak}} \approx 5 \times 10^{23} \text{ erg sec}^{-1}$, where e and m_e are the electron charge and mass, respectively, σ_T is the Thomson cross-section, N is the total number of trapped electrons, d is the distance to the source, and $F_{\nu\text{peak}}$ is the peak-flare flux density.